ISSN 1990-519X, Cell and Tissue Biology, 2018, Vol. 12, No. 3, pp. 247–255. © Pleiades Publishing, Ltd., 2018.
Original Russian Text © P.V. Popryadukhin, G.Y. Yukina, I.P. Dobrovolskaya, E.M. Ivankova, V.E. Yudin, 2017, published in Tsitologiya, 2017, Vol. 59, No. 9, pp. 609–616.

Bioresorption of Porous 3D Matrices Based on Collagen in Liver and Muscular Tissue

P. V. Popryadukhin[a], *, G. Y. Yukina[b], I. P. Dobrovolskaya[c], E. M. Ivankova[a], and V. E. Yudin[c]

[a] *Institute of Macromolecular Compounds, Russian Academy of Sciences, St. Petersburg, 199004 Russia*
[b] *Pavlov First St. Petersburg State Medical University, St. Petersburg, 197022 Russia*
[c] *Peter the Great St. Petersburg Polytechnic University, St. Petersburg, 195251 Russia*
**e-mail: pavel-pn@mail.ru*

Received June 7, 2017

Abstract—Highly porous cylinder-shaped 3D matrices with diameters of 1.3 and 3 mm were obtained by lyophilization of collagen solution. A study in vivo of the mechanism and rate of resorption of the resulting material showed that complete resorption of the matrix occurred 6 weeks after their implantation into liver tissue and 3 weeks after implantation into muscle tissue of animals. Surrounding tissues were not altered or damaged. Histological analysis revealed that, simultaneously with the resorption of matrix collagen, connective tissue and blood vessels were formed. This allows us to recommend the developed porous material based on collagen for use as matrices for tissue engineering and cellular transplantation.

Keywords: 3D porous material, collagen, resorption, tissue engineering, cellular transplantation, liver, muscle tissue, histological analysis

DOI: 10.1134/S1990519X18030094

INTRODUCTION

Tissue engineering, regenerative medicine, and cell transplantation require materials suitable as carriers for cultured cells and biologically active compounds for implantation into living organisms for regeneration of damaged organs and tissue and recovery of lost functions.

The materials should be biocompatible, nontoxic, stable and elastic enough for manipulation in liquid media. They should be capable for resorption in the organism with bioresoption products being not irritating or toxic (Dornish et al., 2001; Gunatillake et al., 2003; Salgado et al., 2004; Dobrovolskaya et al., 2015).

Currently, the most promising materials are ones based on biocompatible, bioresorbable polymers, such as chitosan, alginate, polylactides, polyglycolid, polyhydroxyalkanates, and polyhydroxybutyrate (Dornish et al., 2001; Martinoa et al., 2005; Kohane et al., 2008; Armentano et al., 2010). These polymers are suitable for obtaining film, tubular, spongy, fiber, and nanofiber matrices usable for bioengineering after colonization with stem or somatic cells or saturation with biologically active compounds (Sachlos et al., 2003; Ma et al., 2005; Dobrovolskaya et al., 2016; Ivan'kova et al., 2016). The rate and mechanism of the resorption depend on polymer type and molecular mass, as well as location in the recipient organism (Causa et al., 2007; Bing et al., 2010; Gleadall et al., 2014; Khan et al., 2015).

Tissue bioengineering and transplantology need three-dimensional porous matrices as prototypes of bone tissue and tissue of parenchymatous organs. The implantation of their based tissue engineering product into the living organism is accompanied with two processes: cell migration into the matrix and cell proliferation and differentiation, as well as resorption of the polymer matrix. Successful tissue replacement is possible only with certain ratios of these processes. It should be noted that the matrix destruction by biologically active medium is a complex process depending on many factors (Whu et al., 2013; Popryadukhin et al., 2016).

Collagen is the most promising material for scaffold fabrication (Parenteau-Bareil et al., 2010). It is widely used in medicine for manufacturing of hemostatic, wound-healing, and antiadhesion preparations.

Collagen is a fibrillar protein. It is a major component of the connective tissue in tendons, ligaments, cartilage, bones, and derma, as well as other organs and tissues. In organisms it provides stiffness and elasticity of the connective tissue, has structural and carcass properties. Collagen molecule is a right handed helix (tropocollagen) composed of three α-chains. One turn of the α-chain contains three amino-acid residues. The molecular weight of these molecules

Abbreviations: PCM—porous collagen matrix.

may reach 300 kDa. Tropocollagen is a structural unit of collagen. Tropocollagens are associated into fibrils connected with each other that include covalent bonds. It forms complexly ordered stable structures. In tissues, collagen fibrils combined with each other and other structural proteins generate bundles, collagen fibers with a specific structure and composition depending on the tissue type and organ (Berisio et al., 2002; Shoulders et al., 2009; Chattopadhyay et al., 2014).

Currently, 29 types of collagen are known. They differ in amino-acid sequences, tropocollagen, and fibril structure. Most collagens in the human organism are collagens I, II, III and IV types (Parenteau-Bareil et al., 2010).

In organisms, collagen is destroyed by collagenases. They cleave peptide bonds in certain areas of collagen molecules (Solov'eva, 1998). Under normal conditions, collagenase production is balanced by the synthesis of their inhibitors (tissue metalloproteinase inhibitors) (Yamamoto et al., 1994).

The goal of this study was to develop a porous three-dimensional collagen-based matrix suitable for application in cell transplantation and tissue engineering. This matrix was implanted into muscle and liver tissues of rats and studied for the rate and mechanism of its bioresorption, as well as the surrounding-tissue response and long-term consequences of implantation and resorption.

MATERIALS AND METHODS

Matrix

Porous collagen matrices (PCMs) were fabricated from calf skin (Sigma-Aldrich, United States). Collagen was dissolved in 2% water solution of acetic acid with constant mixing for at least 120 min. Collagen concentration was 3%. The solution was filtered. After removing air at a pressure of 1×10^5 kPa for 3 h, it was frozen at −20°C. The samples were lyophilized at −2°C and 1.6-Pa pressure using Freeze Dry System equipment (United States). Cylindrical samples with 5-mm length, a diameter of 3 mm, and a pore size of from 20 to 200 μm were cut from the blocks using the tubular mill. The samples were converted into water-insoluble forms by holding in vapors of 4% formaldehyde in the phosphate buffer, pH 7.4, for 1 h.

An electron-microscopic study was performed with a Supra 55VP scanning electron microscope (Carl Zeiss, Germany) using the mode of secondary electron registration. The samples were preliminarily coated by a platinum thin layer.

Experiments with Animals

The experiments were done in accordance with the ethical principles for medical research of the European Convention for the Protection of Vertebrate Animals used for Experimental and other Scientific Purposes, Strasbourg, 1986, and World Medical Association Declaration of Helsinki, 1986. Twenty Wistar males of an age of 6 months and weight of 200–250 g were used in experiments.

Cylindrical samples were sterilized in 70% ethanol for 1 h and washed with the excess quantity of the physiological solution. Before surgery, the animals were anesthetized with Zoletil (100–0.1 mL) and Rometar (20 mg/mL, 0.0125 mL per 0.1 kg of animal weight, intraperitoneally). Samples 1.3 mm in size were implanted into the musculus adductor magnus on both pelvic extremities. Three-millimeter matrices were implanted into the same animals into the left lobe of the liver with an outlet less cylindrical hollow made with a tubular mill. Wounds of the extremities and anterior abdominal wall were sutured layer-by layer with Prolen 4-0 thread.

Rats with sutures were kept in individual cells. The animals had free access to water and standard diet composed of PK 120-1 mixed fodder. Animals that had been operated on were active. A negative effect of implantation was not observed. Implantation areas were free from inflammation.

Morphological Evaluation

Muscle and liver tissues with PCM were taken for analysis 1, 2, 3, 6, and 20 weeks (muscle) and 1, 2, 6, and 20 weeks (liver) after implantation. They were fixed in 10% neutral formalin in phosphate buffer (pH 7.4) for at least 24 h, dehydrated in a series of cold ethanols of increasing concentration, and embedded in paraffin blocks by the routine histological technique. Paraffin sections (5 μm) transverse to muscle fibers and PCM transverse to PCM in liver were cut with an Accu-Cut SRT 200 microtome (Sakura, Japan) and stained with Mayer's hematoxylin and eosin (Bio-Optica, Italy). The connective tissue was visualized with Mallory's method (Bio-Optica, Italy). Macrophages and monocytes (mononuclear phagocytes) were identified immunohistochemistry. Anti-CD68 (ab 31630) (Abcam, United Kingdom), dilution 1 : 1000, were used as primary antibodies. Slides were incubated with these antibodies for 1 h at room temperature. The binding of antibodies was revealed with D&A, Reveal-Biotin-Free Polyvalent DAB (Spring Bioscience Corporation, United States). Preparations were stained with Mayer's hematoxylin (Bio-Optica, Italy) and analyzed with a Leica DM750 light microscope (Germany) using ocular 10× and objectives 4×, 10×, 40×, and 100×. Images were captured with ICC50 camera (Leica, Germany).

RESULTS AND DISCUSSION

Figure 1a shows the surface of the PCM transverse section. It is seen that the material has a porous struc-

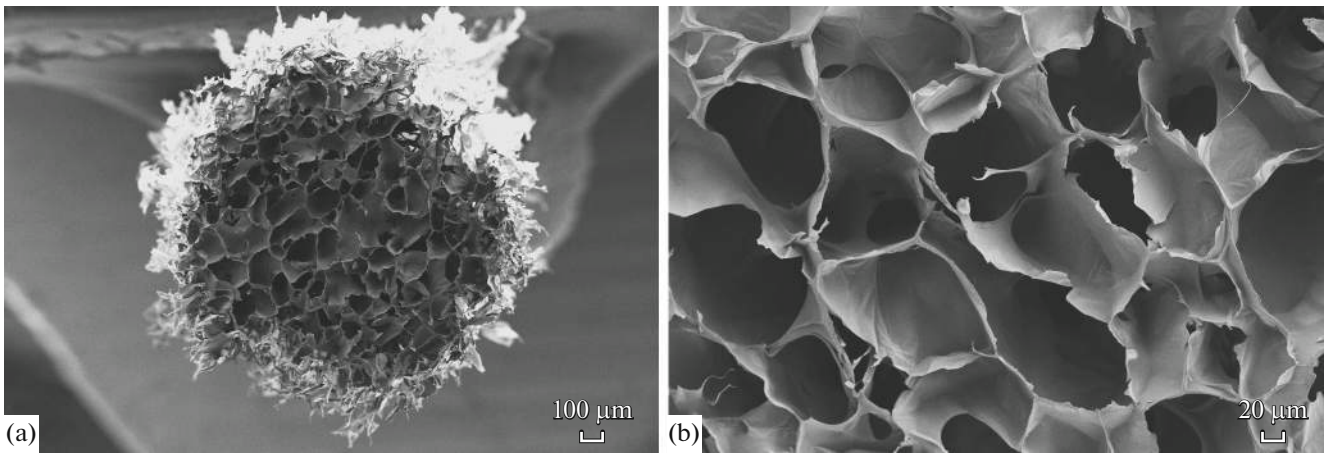

Fig. 1. Cross sections of sponge cylindrical samples of PCM with a diameter of 1.3 mm at various magnifications. Scanning electron microscopy.

ture with an open system of pores connected with each other and the environment. This structure is appropriate for free circulation of nutrients, products of life, and dissolved gasses in the matrix. The pore size and insignificant tortuosity of channels connecting pores promote open cell migration. Application of 3D matrices with similar structures for tissue engineering and cell transplantation has been demonstrated previously (Cheung et al., 2007; Dhandayuthapani et al., 2011, Popryadukhin et al., 2016).

Histological Study of the PCM in 1 Week after Implantation

Figure 2a shows liver 1 week after of PCM implantation. The matrix is inside the tissue and covered outside with a thin layer of connective tissue. The liver color, shape, and size are not altered. Histological investigation revealed moderately severe aseptic inflammation around the PCM. The matrix cross cut has a round shape (Fig. 2b). A capsule of connective tissue with a few thin collagen fibers is formed around the matrix (Fig. 2c). Predominately CD68+ cells, as well as few fibroblasts and giant multinuclear cells, are found in the connective-tissue capsule (Fig. 2d). The peripheral pores of the matrix are filled with numerous CD68+ cells and individual giant multinuclear cells (Figs. 2e, 2f). The central matrix pores contain cellular detritus, erythrocytes, and individual CD68+ cells. No inflammation and dystrophic features are observed in hepatocytes around the matrix.

Morphological assay of the PCM 1 week after implantation showed that it had a round shape in cross sections and was surrounded with a connective-tissue capsule containing mostly CD68+ cells, as well as individual fibroblasts and giant multinuclear cells. In peripheral- and central-matrix pores, CD68+ cells are encountered. No inflammation was observed around the PCM (Figs. 3a, 3b).

Histological Study of the PCM in 2 Weeks after Implantation

In this period, the matrix on the transverse section visibly had a smaller area, and the elongated shape was more compressed compared to the previous period (Fig. 4a). The PCM is surrounded with a thin connective-tissue capsule with a few young collagen fibers and single vessels. The cellular composition of the capsule is represented by fibroblasts, single giant multinuclear cells. The number of CD68+ cells in the capsule is less than in the previous period. Both peripheral and central matrix wells contain CD68+ cells (Figs. 4b, 4c). Fibroblasts are identified only in some peripheral PCM wells. These wells also have thin collagen fibers and individual vessels (Fig. 4d). Hepatocytes around the matrix have no dystrophic changes.

The muscle tissue with PCM in 2 weeks macroscopically looks loose and easily separated into individual bundles, supposedly, due to enhanced activity of collagenases produced by macrophages in the implantation area and decreased amount of native collagen in the connective tissue of the muscle endomysium and perimysium. Similar effect was not observed after implantation of chitosan porous membrane into the rat muscle (Popryadukhin et al., 2016).

The histological testing of PCM in muscles after exposition for 2 weeks showed that the transverse matrix section is visibly smaller than in 1 week after implantation (Fig. 5a). The matrix shape is irregular. A thin capsule with fibroblasts, fibrocytes, CD68+ cells, and single giant multinuclear cells is visible, and no vessels are seen around the matrix. Matrix pores are declined, probably because of a pressure of muscle fibers and low carcass properties of a partially resorbed matrix. All pores of PCM contain CD68+ cells. Signs of inflammation were not revealed around the PCM (Figs. 5b–5d).

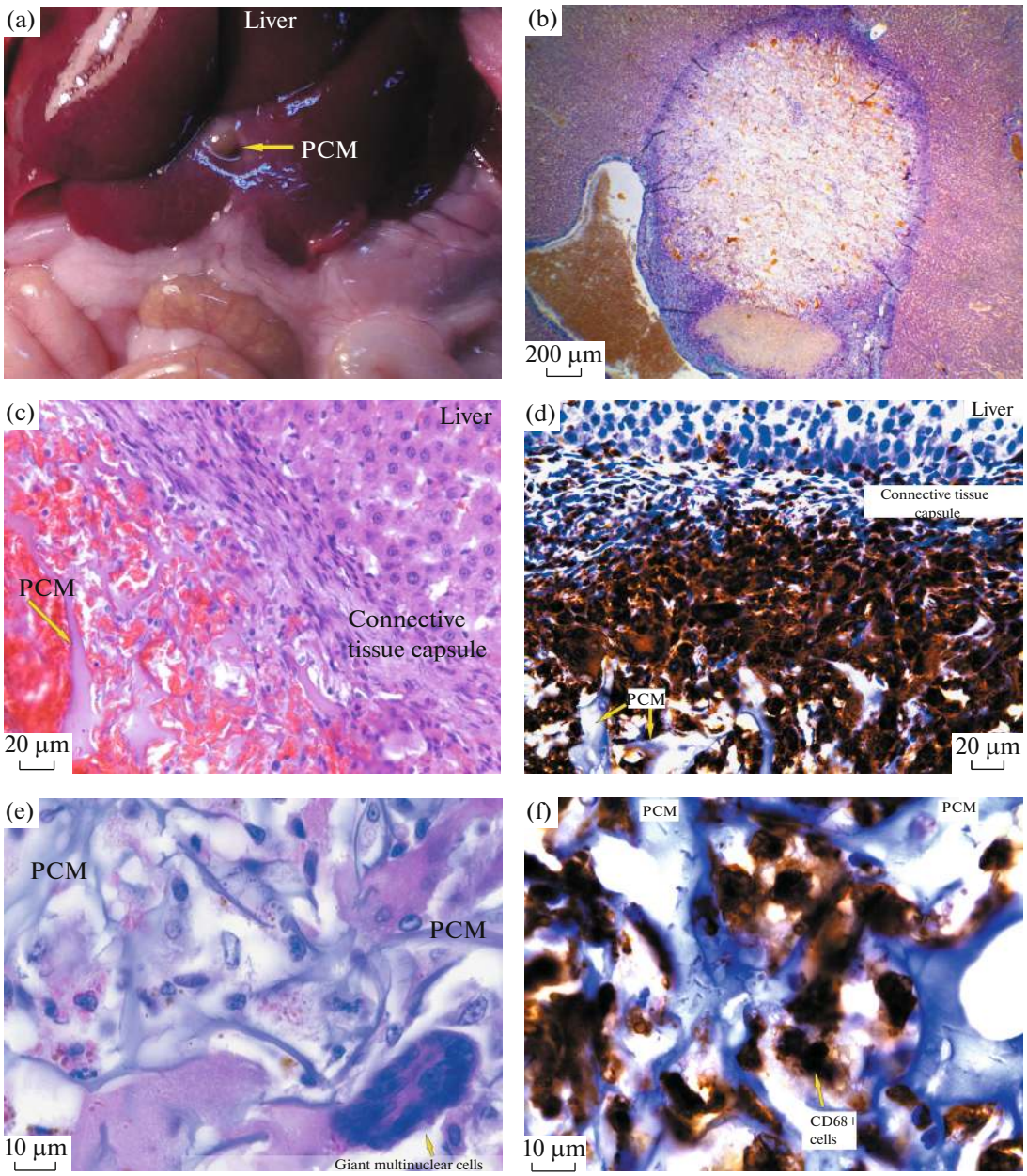

Fig. 2. (a) Rat liver and its histological sections 1 week after PCM implantation. (b) Mallory's staining, ob. 4×; (c, e) hematoxylin/eosin staining, ob. 40× (c), 100× (e); (d, f) immunohistochemical staining of CD68+cells; ob. 40× (d), 100× (f).

Histological Study of the PCM in 3 Weeks after Implantation

Histological analysis of PCM implantation showed that, after 3 weeks, muscle fibers were smooth. No matrix fragments were revealed. The matrix was replaced by connective tissue with fibroblasts, CD68+ cells, and single multinuclear cells. Signs of inflammation in adjacent tissues were not detected (Figs. 6a, 6b).

Histological Study of the PCM in 6 Weeks after Implantation

After 6 weeks, connective tissue with collagen fibers surrounding single fragments of collaged matrix was seen at the site of PCM implantation (Fig. 7a). The cellular composition was represented by fibroblasts, fibrocytes, CD68+ cells, giant multinuclear cells, and a few lymphocytes. Apoptotic bodies were not revealed. Vessels penetrating the connective tissue were widened and full of blood (Figs. 7b–7d).

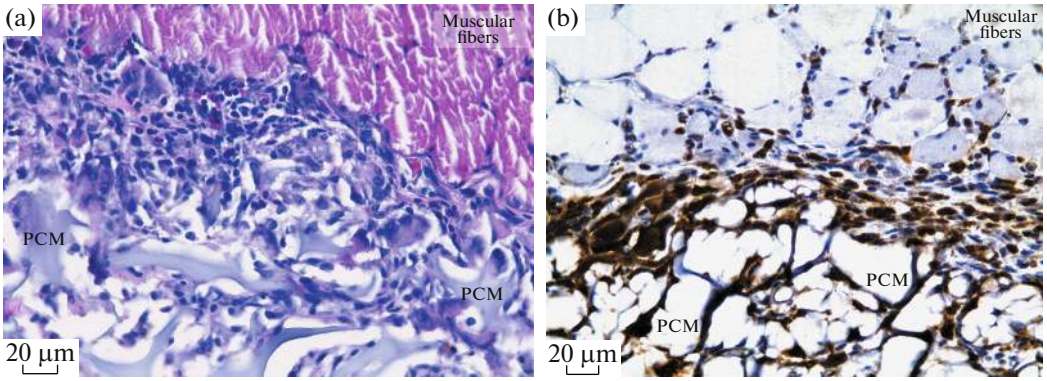

Fig. 3. Histochemical sections of rat-muscle tissue in 1 week after PCM implantation. Hematoxylin/eosin staining, ob. 40×; (b) immunohistochemical identification of CD68+ cells, ob. 40×.

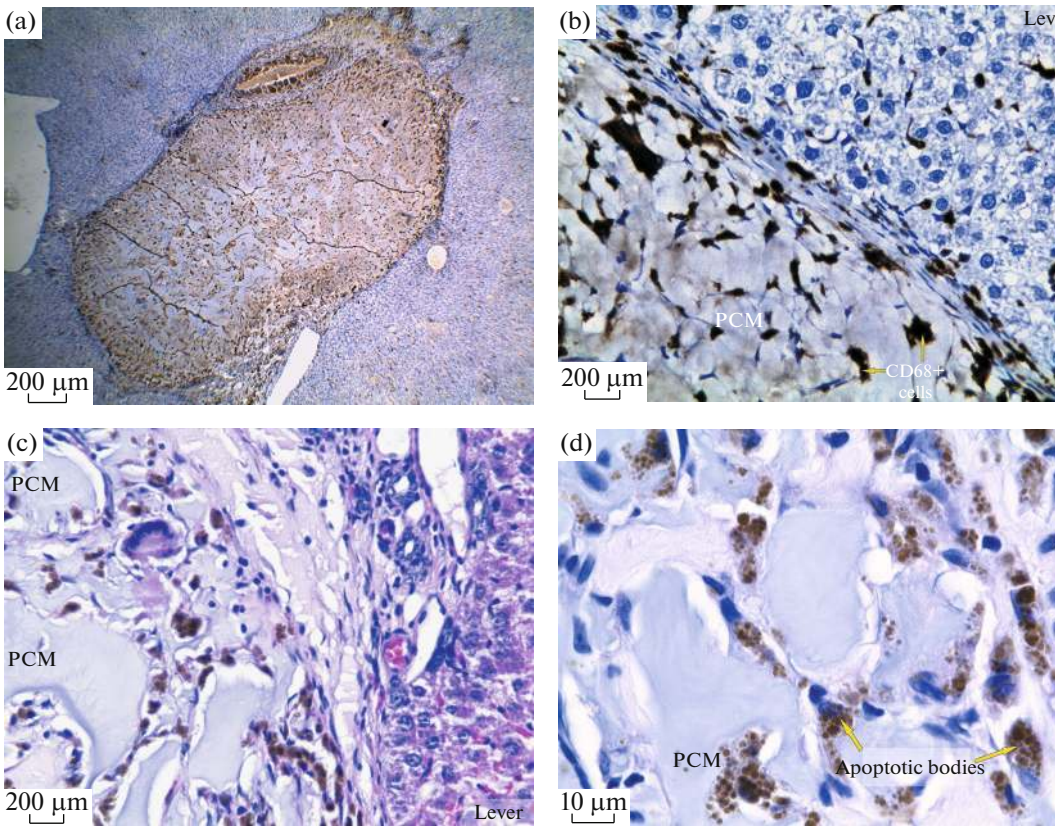

Fig. 4. Histochemical sections of rat-liver tissue 2 weeks after PCM implantation. (a, b, d) immunohistochemical identification of CD68+ cells, ob. (a) 4×, (b) 40×, and (d) 100×; (c) hematoxylin/eosin staining, ob. 40×.

Hepatocytes surrounding the matrix were free of dystrophic changes.

Macroscopic investigation of muscles revealed that the tissue was loose, as in the previous experimental period. The PCM was not identified morphologically. Connective tissue with fibroblasts and CD68+ cells were seen at the location of the matrix.

Histological Study of the PCM in 20 Weeks after Implantation

Twenty weeks after PCM implantation into the liver, its color, shape, and size as a whole were not altered. The adhesive process was not revealed. A star-like scar was observed at the implantation site (Fig. 8a). The area occupied with the connective tis-

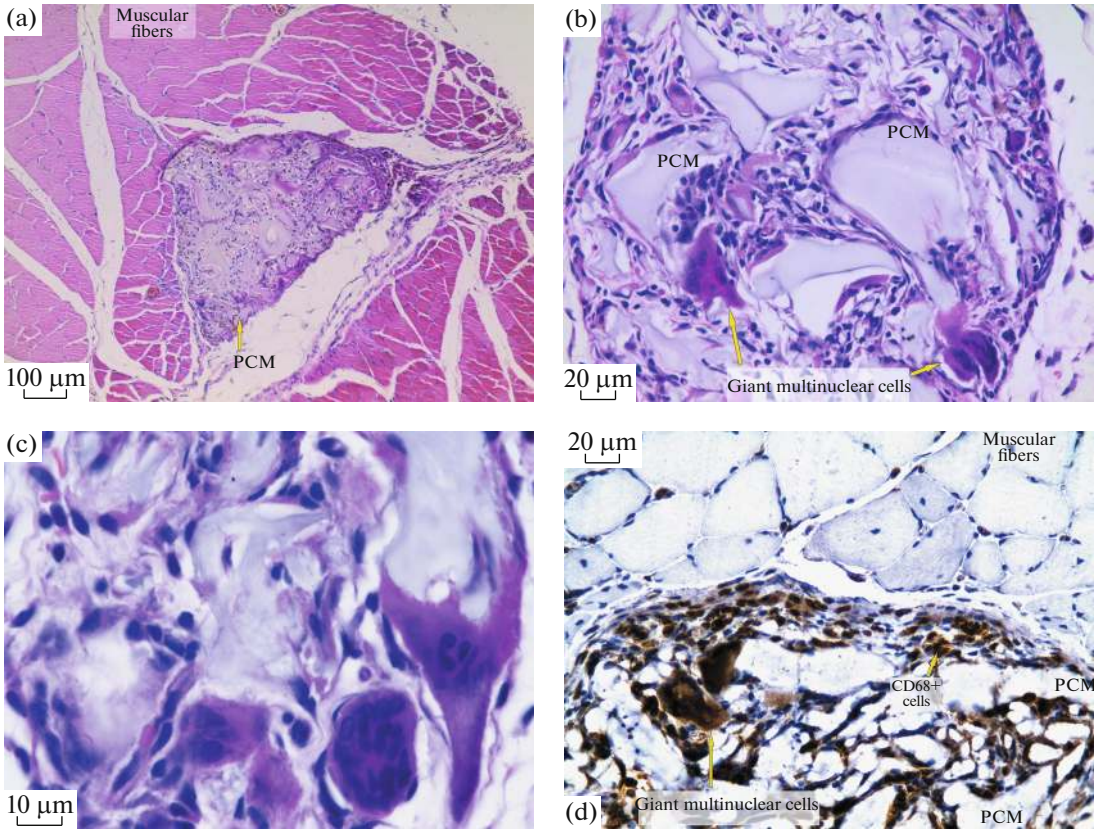

Fig. 5. Histochemical sections of rat-muscle tissue in 2 weeks after PCM implantation. (a–c) Hematoxylin/eosin staining, ob. (a) 10×, (b) 40×, and (c) 100×; (d) immunohistochemical identification of CD68+ cells, ob. 40×.

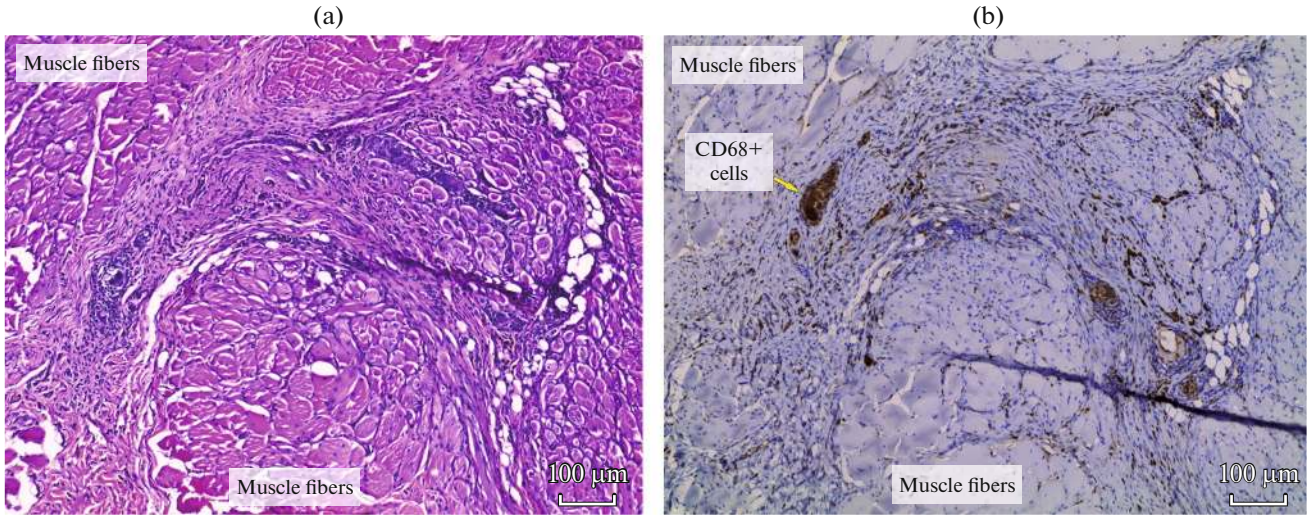

Fig. 6. Histological sections of rat-muscle tissue in 3 weeks after PCM implantation. (a) Hematoxylin/eosin staining, ob. 10×; (b) immunohistochemical identification of CD68+ cells, ob. 10×.

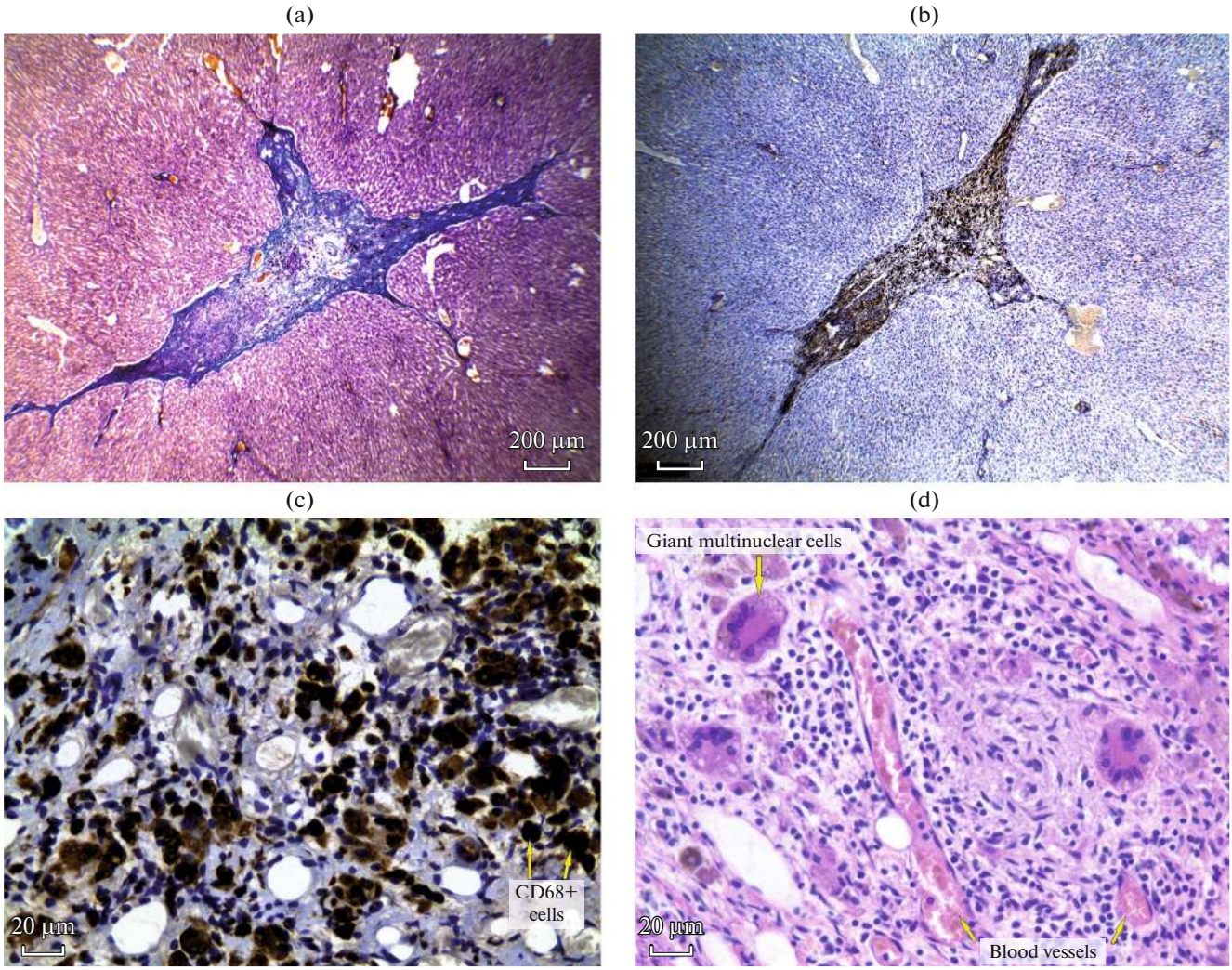

Fig. 7. Histological sections of rat-liver tissue in 6 weeks after PCM implantation. (a) Mallory's staining, ob. 4×; (b, c) immunohistochemical identification of CD68+ cells, ob. (b) 4× and (c) 40×; (d) hematoxylin/eosin staining, ob. 40×.

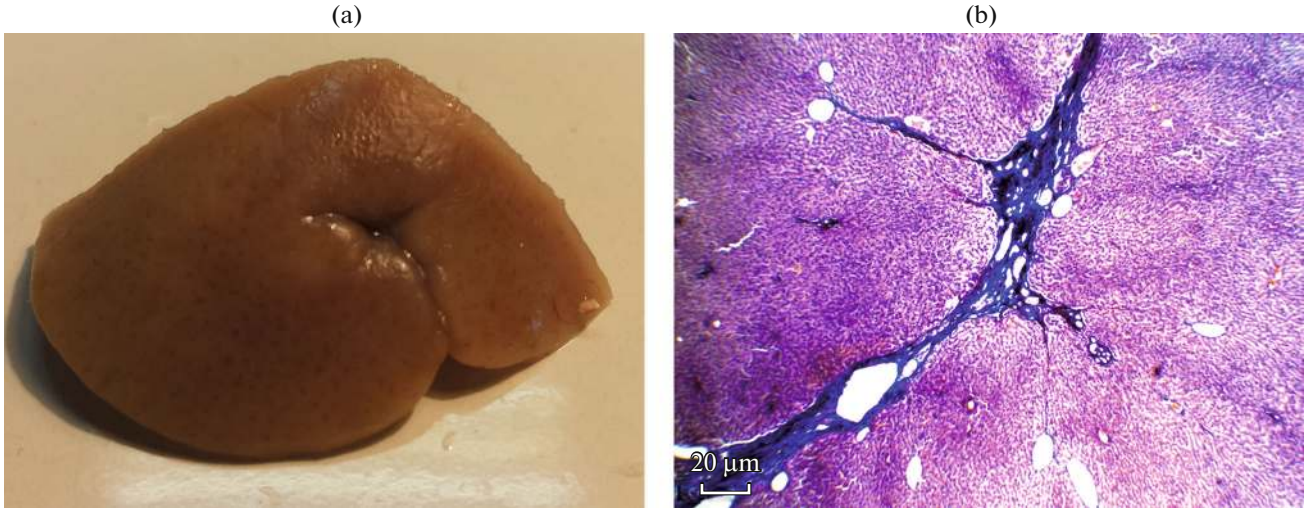

Fig. 8. General view of the liver fixed with 10% formalin for 24 h. (a) Histological section of rat-liver tissue with Mallory's staining, ob. 4×; (b) in 20 weeks after PCM implantation.

sue was visibly smaller than at 6 weeks after implantation (Fig. 8b). No matrix fragments were detected.

In this period, no connective tissue scars were revealed in the muscle tissue at the site of PCM implantation. Muscle fibers had no sign of damage and generated dense bundles.

Thus, it has been demonstrated morphologically that PCM replacing muscle and liver defects caused a weak inflammatory process only on the early period after implantation. At late periods, it was not observed. The matrix implantation did not produce dystrophic changes in hepatocytes and muscle fibers. PCM resorption takes place with the active participation of CD68+ cells. Mononuclear phagocytes penetrate into all matrix wells before fibroblasts. After performing their function, CD68+ cells die by apoptosis. In active phagocytotic processes, fibroblasts in the liver populate only individual peripheral pores in the matrix. It prevents the growth of blood vessels inside the matrix. The bioresorption of the matrix in liver is completed after 6-week exposure.

In muscles, the PCM drastically reduced in volume as a result of CD68+ cell activity and the pressure of muscle fibers, and in 3 weeks its fragments were not revealed.

Thus, CD68+ cells play a key role in PCM degradation. Macrophages and giant multinuclear cells are the first to fill the pore volume and actively phagocyte the matrix material. The PCM did not grow with the connective tissue and vessels, because the matrix bioresorption occurs more rapidly than its fibroblast migration.

After the bioresorption process is completed in the liver, scar tissue is not identified in muscles.

The results of this study show that PCM may be recommended to obtain short-term bioengineering products for their application in regenerative medicine and cell transplantation.

ACKNOWLEDGMENTS

This study was supported by the Russian Science Foundation, project no.14-33-00003.

REFERENCES

Armentano, I., Dottori, M., Fortunati, E., and Kenny, J.M., Biodegradable polymer matrix nanocomposites for tissue engineering: a review, *Polym. Degrad. Stab.*, 2010, vol. 95, no. 11, pp. 2126–2146.

Berisio, R., Vitagliano, L., Mazzarella, L., and Zagari, A., Crystal structure of the collagen triple helix model [(Pro–Pro–Gly)10]3, *Protein Sci*, 2002, vol. 11, no. 2, pp. 262–270.

Bing, Y., Xing, Y.L., Shuai, S., Xiang, Y.K., Gang, G., Mei, J.H., Feng, L., Yu, Q.W., Xia, Z., and Zhi, Y.Q., Preparation and characterization of a novel chitosan scaffold, *Carbohydr. Polym.*, 2010, vol. 80, pp. 860–865.

Causa, F., Netti, P.A., and Ambrosio, L., A Multi-functional scaffold for tissue regeneration: the need to engineer a tissue analogue, *Biomaterials*, 2007, vol. 28, no. 34, pp. 5093–5099.

Chattopadhyay, S. and Raines, R.T., Collagen-based biomaterials for wound healing, *Biopolymers*, 2014, vol. 101, no. 8, pp. 821–833.

Cheung, H., Lau, K., Lu, T., and Hui, D., A critical review on polymer-based bio-engineered materials for scaffold development, *Composites, Part B: Engineering*, 2007, vol. 38, no. 3, pp. 291–300.

Dhandayuthapani, B., Yoshida, Y., Maekawa, T., and Kumar, D.S., Polymeric scaffolds in tissue engineering application: a review, *Int. J. Polymer Sci.* 2011, Article ID 290602.

Dobrovol'skaya, I.P., Popryadukhin, P.V., Yudin, V.E., Ivan'kova, E.M., Yukina, G.Yu., Yudenko, A.N., and Smirnova, N.V., Biological resorption of fibers from chitosan in endomysium and perimysium of muscular tissue, *Cell Tissue Biol.*, 2016, vol. 10, no. 5, pp. 395–401.

Dobrovolskaya, I.P., Popryadukhin, P.V., Yudin, V.E., Ivan'kova, E.M., Elokhovskiy, V.Yu., Weishauptova, Z., and Balik, K., Structure and properties of porous films based on aliphatic copolyamide developed for cellular technologies, *J. Mater. Sci. Mater. Med.*, 2015, vol. 26, no. 1, pp. 5381–5391.

Dornish, M., Kaplan, D., and Skaugrud, O., Standards and guidelines for biopolymers in tissue-engineered medical products, *Ann. NY Acad. Sci.*, 2001, vol. 944, pp. 388–397.

Gleadall, A., Pan, J., Kruft, M.-A., and Kellomäki, M., Degradation mechanisms of bioresorbable polyesters, part 2. Effects of initial molecular weight and residual monomer, *Acta Biomat.*, 2014, vol. 10, pp. 2233–2240.

Gunatillake, P.A. and Adhikari, R., Biodegradable synthetic polymers for tissue engineering, *Eur. Cell. Mater.*, 2003, vol. 20, pp. 1–16.

Ivan'kova, E.M., Dobrovolskaya, I.P., Popryadukhin, P.V., Kryukov, A., Yudin, V.E., and Morganti, P., In-situ cryo-SEM investigation of porous structure formation of chitosan sponges, *Polym. Test.*, 2016, vol. 52, pp. 41–45.

Khan, F., Tanaka, M., and Ahmad, S.R., Fabrication of polymeric biomaterials: a strategy for tissue engineering and medical devices, *J. Mater. Chem. B*, 2015, vol. 3, pp. 8224–8249.

Kohane, D.S. and Langer, R., Polymeric biomaterials in tissue engineering, *Pediatr. Res.*, 2008, vol. 63, no. 5, pp. 487–491.

Ma, Z., Kotaki, M., Inai, R., and Ramakrishna, S., Potential of nanofiber matrix as tissue-engineering scaffolds, *Tissue Eng.*, 2005, vol. 11, no. 1–2, pp. 101–109.

Martinoa, Di, A., Sittinger, M., and Risbud, M.V., Chitosan: a versatile biopolymer for orthopaedic tissue-engineering, *Biomaterials*, 2005, vol. 26, pp. 5983–5990.

Parenteau-Bareil, R., Gauvin, R., and Berthod, F., Collagen-based biomaterials for tissue engineering applications, *Materials*, 2010, vol. 3, pp. 1863–1887.

Popryaduhin, P.V., Yukina, G.Yu., Suslov, D.N., Dobrovolskaya, I.P., Ivankova, E.M., and Yudin, V.E., Bioresorption of porous 3D-materials based on chitosan, *Tsitologiia*, 2016, vol. 58, no. 10, pp. 771–777.

Sachlos, E. and Czernuszka, J.T., Making tissue engineering scaffolds work. Review on the application of solid

freeform fabrication technology to the production of tissue engineering scaffolds. Making tissue engineering, *Eur. Cell. Mater.*, 2003, vol. 5, pp. 29–40.

Salgado, A.J., Coutinho, O.P., and Reis, R.L., Bone tissue engineering: state of the art and future trends, *Macromol. Biosci.*, 2004, vol. 4, pp. 743–765.

Shoulders, M.D. and Raines, R.T., Collagen structure and stability, *Annu. Rev. Biochem.*, 2009, vol. 78, pp. 929–958.

Solov'eva, N.I., Matrix metalloproteinases and their biological functions, *Bioorg. Khim.*, 1998, vol. 24, no. 4, pp. 245–255.

Whu, S.W., Hung, K., Hsieh, K., Chen, C., Tsai, C., and Hsu, S., In vitro and in vivo evaluation of chitosan–gelatin scaffolds for cartilage tissue engineering, *Mat. Sci. Eng.*, 2013, vol. 33, pp. 2855–2863.

Yamamoto, M., Sawaya, R., Mohanam, S., Loskutoff, D.J., Bruner, J.M., Rao, V.H., Oka, K., Tomonaga, M., Nicolson, G.L., and Rao, J.S., Expression and localization of urokinase-type plasminogen activator receptor in human gliomas, *Cancer Res.*, 1994, vol. 54, pp. 3329–3332.

Translated by I. Fridlyanskaya